

# Laser Beam Tracking by Repetitive And Variable-Order Adaptive Control

Chi-Ying Lin, Yen-Cheng Chen, Tsu-Chin Tsao, and Steve Gibson

**Abstract**—This paper addresses laser beam tracking control problem for tracing dynamic trajectories subject to random disturbances. A variable-order adaptive control scheme based on a recursive least-squares lattice filter is applied for suppressing random jitter. For tracking a reference trajectory generated by a deterministic dynamic model, an internal model principle based feedback loop is introduced as an outer loop to the adaptive feedback loop to achieve asymptotic tracking performance. Particularly a repetitive control is applied to track periodic trajectories. A feature of the control system proposed in this paper is that the design of the adaptive and repetitive control are independent because each design is based only on the plant model. Experiment conducted on a two-axis fast steering mirror for tracking diamond-shaped beam path demonstrates the ability of the integrated control to achieve asymptotic tracking of periodic trajectories by the repetitive control while optimally rejecting random disturbances by the adaptive control.

## I. INTRODUCTION

Precise laser beam tracking of dynamic trajectories with high-bandwidth rejection of disturbances produced by platform vibration and atmospheric turbulence are critical to applications such as high-energy laser systems, laser based medical operations, and laser cutting and welding. The laser beam is required to generate deterministic trajectories, for example, projectile motion, raster scan traces, or manufactured part contours subject to jitter sources composed of random disturbances with multiple bandwidths coming from platform vibration filtered by lightly damped structural modes, atmospheric turbulence, and laser plumes in the beam path. The actuator used to steer laser beams are typically electromechanical, MEMS-based fast steering mirrors, or more recent liquid crystal optical phased arrays.

Effective control systems for above mentioned applications should address the deterministic nature of the tracking problem and the random and time varying characteristic of the disturbance rejection problem, where the actuator dynamics are usually time invariant and identified a priori. This motivates us to propose a control system, which applies the internal model principle for asymptotic tracking and adaptive control for rejection of time varying stochastic disturbances.

Recent research on jitter control has produced adaptive control methods that employ least-mean-square (LMS) [1]–

This work was supported by the U.S. Air Force Office of Scientific Research under Grant F49620-02-01-0319 and the U.S Naval Office of Research under Grant N00014-07-1-1063.

The authors are with the Mechanical and Aerospace Engineering Department, University of California, Los Angeles 90095-1597, chiying@seas.ucla.edu, yencheng@ucla.edu, ttsao@seas.ucla.edu, gibson@ucla.edu.

[3] adaptive filtering and recursive least-squares (RLS) adaptive filtering [4]–[6]. The trade off is between a simpler algorithm (hence computational economy) with LMS versus faster convergence and exact minimum-variance steady-state performance with RLS. The RLS based adaptive control compensates for both random and deterministic disturbances by minimizing the RMS value of the output with respect to a fixed order FIR filter. Due to the averaging nature of the RMS value, the adaptive control's high frequency tracking performance is sometimes less desirable as short duration large error could still exist for minimized RMS value. In many applications, the laser beam is required to generate traces that in the time domain are represented by periodic signals in each axis. This motivates the use of repetitive control, which includes the periodic signal dynamics in the feedback loop based on the internal model principle. Repetitive controls by stable inversion approach [7], [8] or by robust performance design [9] have been shown to be effective for motion control applications. However, broadband frequency components are usually present in the laser beam system.

Utilizing Youla-parametrization (internal model control) control structure, the design and parametrization of these two control actions can be made to be independent of each other but dependent only on the a priori identified plant dynamics. The superior performance achieved by the synergy of the adaptive and repetitive control schemes that is not achievable by individual adaptive or repetitive control scheme will be demonstrated by experimental results.

The experiment described in this paper is similar to that used for [4]–[6], [10], but the fast steering mirror used as the control actuator here has very different dynamics from that of the MEMS mirror used for [5], [6], [10]. Because of this difference and the complex jitter profile used for the experiments reported here, the closed-loop performance benefits from much higher adaptive-filter orders than those used in [4]–[6], [10].

Section II describes the experimental system. Section III describes the design of the control system, which consists of linear time-invariant (LTI) feedback loops augmented by the adaptive control and repetitive control loops. Experimental results are presented in Section IV followed by concluding remarks given in Section V.

## II. DESCRIPTION OF THE EXPERIMENTAL SYSTEM

The main components of the beam steering experiment, shown in Fig. 1 and its representative block diagram depicted



Fig. 1. UCLA laser beam steering experiment. Upper left: laser source. Upper right: FSM 1, disturbance actuator. Lower right: FSM 2, control actuator, mounted on shaker. Lower left: optical position sensor.

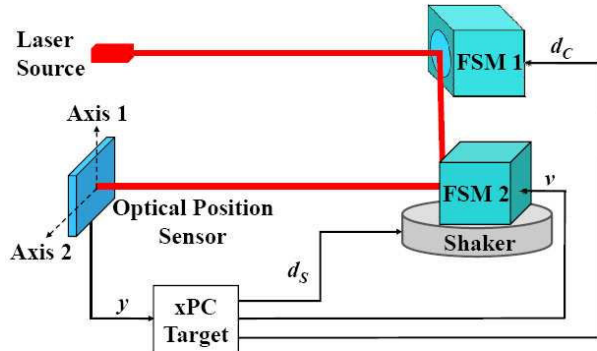


Fig. 2. Diagram of the experiment.

in Fig. 2, are a 635nm laser, two Fast Steering Mirrors (FSM 1 and FSM 2), and an On-Trak optical position sensor (OPS) that tracks the position of the image that the laser beam forms on the plane of the sensor. The two-dimensional vector  $y$  denotes the measured position of the laser spot. The steering mirror labeled FSM 2 is used as the control actuator and is driven by a control sequence  $v$ , while the mirror labeled FSM 1 is used to add disturbance to the beam, and is driven with a designed disturbance sequence  $d_M$ . The beam path between the control actuator FSM 2 and the optical position sensor is 1 meter so 1 mm displacement on the OPS corresponds to 1 milli-radians beam angle change when the beam emits from a fixed point in FSM 2.

The control actuator FSM 2 is a Newport model FSM-200 mirror, which includes differential impedance transducers and an internal analog feedback control loop for angular stabilization of the mirror. This internal feedback loop remained turned on for all experiments reported in this paper, so that the digital adaptive and optimal control loops used here augment the existing internal control loop. The disturbance generator FSM 1 is a Newport model FSM-100 mirror.

The control, disturbance and measurement sequences are processed in real-time using MATLAB's xPC software with a stand alone target machine operating at a sample-and-hold rate of 2kHz. In order to inject a wider variety of disturbances the control actuator was mounted on top of a

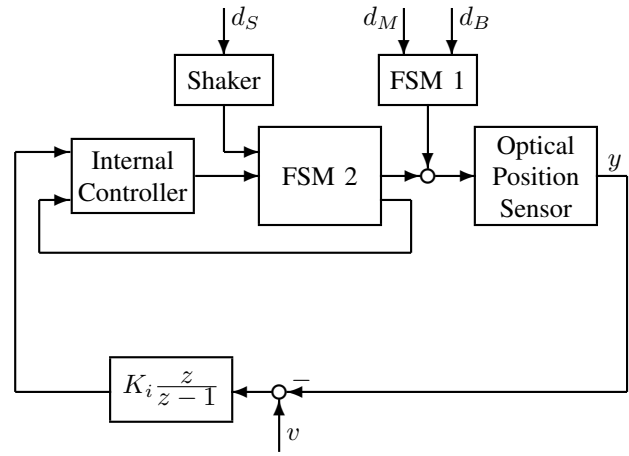


Fig. 3. Block diagram of the plant model including the LTI integrator feedback loop.  $d_S$  = disturbance command to shaker;  $d_M$  = disturbance command to FSM 1;  $d_B$  = building vibration;  $a_S$  = acceleration produced by shaker;  $\hat{w}$  = estimated combined disturbance.

shaker which was commanded with a desired disturbance sequence  $d_S$  to the amplifier and generated vibration in the vertical direction. This vertical vibration excites motion in both angular axes of the control mirror. As can be expected, the effect is stronger on the optical position sensor Axis 2 than Axis 1. Furthermore, although unintentionally, the test bench was exposed to a third disturbance source, the building floor vibration.

### III. CONTROL SYSTEM

#### A. LTI Feedback Loops

The Newport fast steering mirror denoted as FSM 2 is the actuator for the beam control system. The mirror has an analog control loop that feeds back internal measurements of the position of the mirror relative to its case. This loop effectively stabilizes the mirror's torsional vibration mode at approximately 10 Hz. The internal feedback controller can be disengaged and replaced by a feedback loop of the users' choice. However, a goal of this paper is to demonstrate that the adaptive controller can be used to augment whatever stabilizing LTI feedback controller is already in place. Hence, the internal controller was not replaced with a high-performance robust feedback loop similar to any of those used in [4], [6], [10]. Only an integral feedback of the beam position error was added to the internal feedback loop, as shown in Fig. 3. Hence, there are two LTI feedback control loops: the internal controller and the integrator loop.

The integrator gain  $K_i$  was chosen to maximize the error-rejection bandwidth without amplifying high-frequency disturbance. The closed-loop transfer function, from  $u$  to  $y$ , which includes the internal feedback loop and the integrator loop will be referred to as  $G(z)$  in following sections.

#### B. Adaptive Control Loop

In typical beam-steering applications the dynamic models of the fast steering mirrors either are known or can be determined by a one-time identification. The disturbance

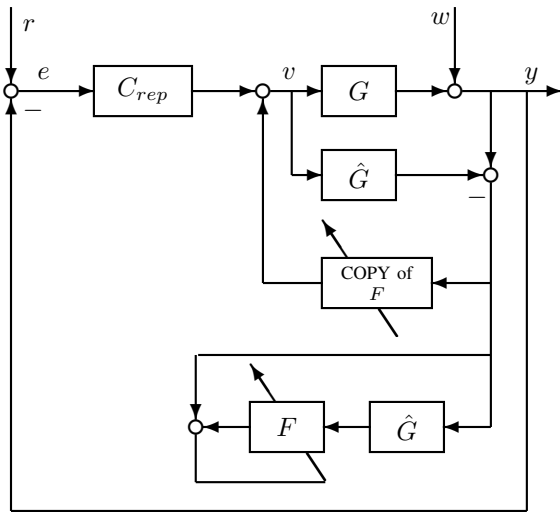


Fig. 4. Block diagram of the control system with adaptive and repetitive control.

characteristics, however, depend on the atmospheric conditions in the optical paths and on the excited vibration modes of the structures on which the optical systems are mounted, so that the disturbance characteristics commonly vary during operation of a beam steering system. Therefore, the adaptive control algorithm presented in this paper assumes known LTI plant dynamics but unknown disturbance dynamics.

To model the random disturbance inputs, the various jitter sources are convolved with the transfer functions from those sources to the output error, with the LTI feedback loops closed, to produce the net jitter that the adaptive loop controls. The jitter model is represented as an output disturbance in an innovations state-space form:

$$\begin{aligned} zx_W &= A_W x_W + B_W \varepsilon \\ w &= C_W x_W + \varepsilon \end{aligned} \quad (1)$$

where  $\varepsilon$  is a zero-mean, stationary, white-noise sequence, and the matrix  $B_W$  is a Kalman predictor gain. The jitter model  $\hat{W}(z)$  has both zeros and poles strictly inside the unit circle.

It follows from well known results on linear optimal control that, when  $(G = \hat{G})$  holds, the optimal controller can be parameterized as in Fig. 4 where  $F$  is a stable LTI filter. It follows that the steady-state variance of  $y$  is equal to square of the performance index

$$J_2 = \|(I + GF)W\|_2 \|\varepsilon\|_2 \quad (2)$$

where  $\|\cdot\|_2$  is the  $H_2$  norm for stable LTI systems, and  $\|\varepsilon\|_2$  is the standard deviation of  $\varepsilon$  (a constant independent of the controller). The adaptive control implicitly identifies the disturbance dynamics and minimizes the variance of the position error  $y$  in Fig. 4, wherein it is treated that  $C_{rep}=0$ . The minimization being over controllers having the structure of the adaptive loop in Fig. 4 with an FIR filter  $F(z)$  of order  $N$ .

The adaptive controller requires an estimate  $\hat{G}(z)$  of the closed-loop transfer function from the adaptive control command to the measured beam position error  $y$ , without the adaptive loop closed. The RLS lattice filter in the adaptive control loop tracks the statistics of the disturbance and identifies gains to minimize the RMS value of the possibly noisy output error signal  $y$ .

The adaptive FIR lattice filter  $F(z)$  is the main component of the adaptive controller. In this paper, the two-channel reference signal, or input to  $F(z)$ , is constructed from the two-axis output error  $y$ , as indicated in Fig. 4. The tuning signal for the adaptive filter also is  $y$ . Because of the multichannel nature of the lattice filter, the adaptive control algorithm can accommodate additional signals, such as accelerometer measurements [11], [12]. For the results presented in this paper, the two channels of the adaptive controller were uncoupled, although the adaptive lattice filter permits the use of multiple sensor channels for generating the command for each control channel.

The details of the lattice-filter algorithms used here are beyond the scope of this paper. These algorithms are reparameterized versions of algorithms in Jiang and Gibson [13]. The current parameterization of the lattice algorithms is optimized for indefinite real-time operation. The current lattice filter maintains two important characteristics of the RLS lattice filter in Jiang and Gibson [13]: channel orthogonalization, which is essential to numerical stability in multichannel applications, and the unwrapped property of the lattice filter, which is essential to rapid convergence.

In addition to the disturbance rejection when reference tracking is also considered for the adaptive control, the reference signal  $r$  enters the adaptive control loop similar to the disturbance  $w$  as suggested in Fig. 2. In this case the reference signal, like the disturbance signal, is considered as a stochastic process. Since in many applications, the reference signals, such as harmonic and periodic signals, can be generated by deterministic dynamics, it is possible to achieve asymptotic tracking by applying the internal model principle. Particularly it will be useful to integrate a repetitive control loop for tracking periodic references with the above formulated adaptive control.

### C. Repetitive Control

The integrated adaptive and repetitive control is shown in Fig. 4, where  $C_{rep}$  is the repetitive controller. If  $(G = \hat{G})$ , the transfer function from the reference signal  $r$  and disturbance  $w$  to the error signal  $e$  is

$$e = \frac{1}{1 + \hat{G}C_{rep}} r - \frac{1 + \hat{G}F}{1 + \hat{G}C_{rep}} w \quad (3)$$

This compares to the case that only the adaptive control is applied, where the reference  $r$  is treated similar to the disturbance  $w$ :

$$e = (1 + \hat{G}F)w - (1 + \hat{G}F)r \quad (4)$$

The repetitive controller  $C_{rep}$ , can be considered as a plug-in to the adaptive control and is designed based on the LTI closed loop plant model  $\hat{G}$ , disregarding the adaptive filter  $F$ . When only repetitive control is realized, The adaptive filter  $F(z) = 0$ . For the integrated adaptive and repetitive control, both the adaptive filter  $F$  and the fixed repetitive controller  $C_{rep}$  are active.

The repetitive controller includes an internal model and is in the following filter from [7], [8]:

$$C_{rep} = \frac{q(z, z^{-1})z^{-N_p+l}}{1 - q(z, z^{-1})z^{-N_p}} K_{rep}(z) \quad (5)$$

$N_p$  stands for the period of the reference signal,  $l$  is the sum of the plant delay and the controller delay which comes from the inversion of the unstable zero part in the closed loop plant  $\hat{G}$ .  $q(z, z^{-1})$  is a zero phase low pass filter for establishing robust stability in the following form:

$$q(z, z^{-1}) = (az^{-1} + b + az)^p \quad (6)$$

where  $a$  &  $b$  satisfies  $a + 2b = 1$  for unity d.c. gain and  $p$  is a positive integer.

$K_{rep}(z)$  can be obtained by a zero phase error compensation [7] as an approximate stable inversion of  $\hat{G}$ , or from robust control approaches by formulating and solving a  $\mu$ -synthesis problem [9]. Although  $q(z, z^{-1})$  is a non-causal filter, the controller's causality is still assured because of the cascaded long delay terms  $z^{-N_p}$  and  $z^{-N_p+l}$ .

#### IV. EXPERIMENTAL RESULTS

In the experimental results presented below the laser beam control is to track periodic reference trajectories of 0.05 second period interval for each of the two axes shown in Fig. 5. These reference signals make a diamond-shaped profile in the XY coordinate frame. The Fourier harmonics of the periodic trajectories clearly stand out in the spectrum plot in Fig. 5 at the frequencies  $(20 + 40k)$  Hz,  $k \in \mathbf{Z}$ . The spectral contents of the disturbances injected to the shaker and the mirror FSM 1 as well as the low frequency building vibration are shown in Fig. 6. These disturbance signals, which correspond to  $w$  in Fig. 2, were acquired from the experimental output responses with the LTI feedback loop closed when the reference was set to zero. As can be seen the disturbance spectra contain two broad bandwidth humps and a number of narrow bandwidth signals at various frequencies where some of them coincide with the integer multiples of 20 Hz.

Two groups of experiment, one without and one with the random disturbance input injected, will be shown. All the controllers are based on the plant model ( $\hat{G}$ ), which contains the LTI integrator feedback loop. In each group, the results of three control schemes, first with the adaptive control only, second with the repetitive control only, and finally with both the adaptive and repetitive control applied, are presented. The adaptive lattice filter in the experiment was of 30th order.

The steady state tracking error of each of the six cases are shown in Fig. 7. Without the random disturbance, the

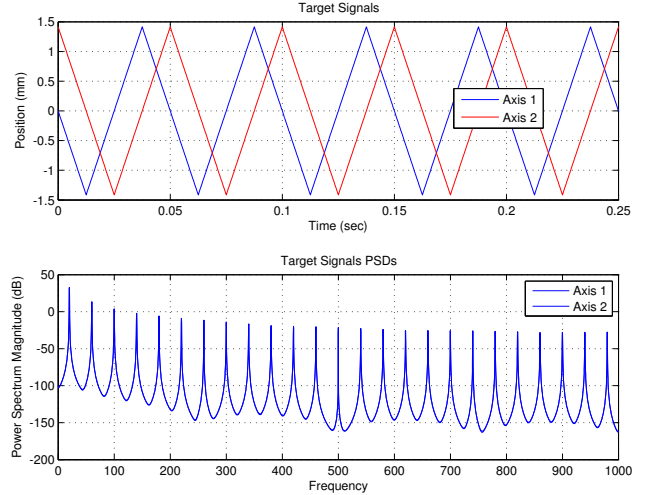


Fig. 5. 20 Hz triangular wave tracking profile. (blue: 1st axis; red: 2nd axis). Upper: time domain; lower: frequency domain.

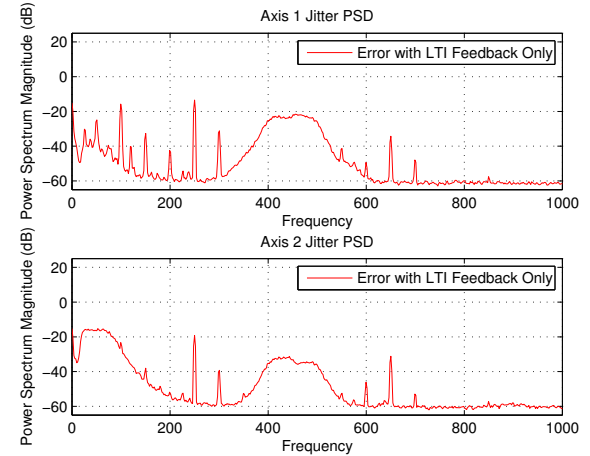


Fig. 6. Disturbance Power Spectral Density. (blue: 1st axis; red: 2nd axis). Upper: time domain; lower: frequency domain.

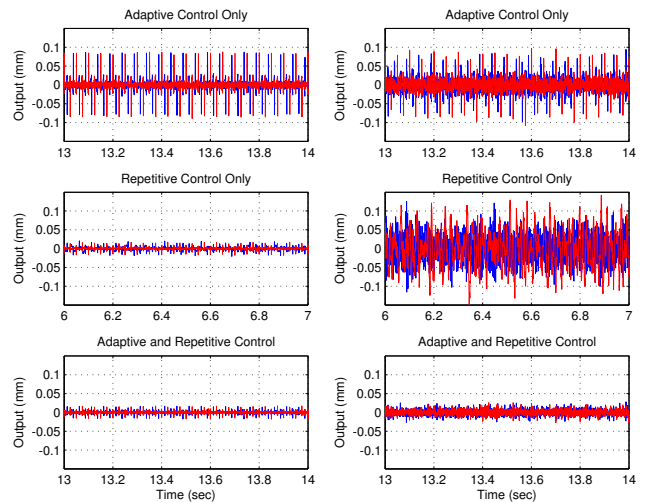


Fig. 7. Tracking error steady state performance for each axis (blue: 1st axis; red: 2nd axis). Upper left: adaptive control without disturbance; upper right: adaptive control with disturbance; middle left: repetitive control without disturbance; middle right: repetitive control with disturbance; lower left: adaptive + repetitive control without disturbance; lower right: adaptive + repetitive control with disturbance.

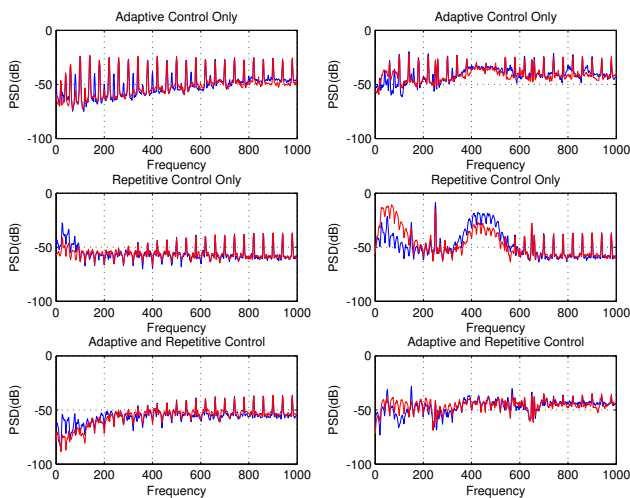


Fig. 8. Power spectrum of the steady state tracking error (blue: 1st axis; red: 2nd axis). Upper left: adaptive control without disturbance; upper right: adaptive control with disturbance; middle left: repetitive control without disturbance; middle right: repetitive control with disturbance; lower left: adaptive + repetitive control without disturbance; lower right: adaptive + repetitive control with disturbance.

adaptive control performs reasonable well for tracking. The repetitive control, however, shows even smaller error. When the random disturbance is present, the adaptive control rejects the disturbance by minimizing the output variance. As the plot shows, the repetitive control is not capable of rejecting the random disturbance, but the repetitive and adaptive control together achieves superior performance. The power spectra of the steady state error signals shown in Fig. 8 further elucidate the comparisons and synergy. Clearly the adaptive control suppresses the two broad bandwidth humps but significant narrow band spikes remain. The repetitive control suppresses the Fourier harmonic frequencies at integer multiples of 20 Hz for up to about 400 Hz, beyond which the repetitive control is inactive due to the bandwidth of the filter  $Q$ . The adaptive and repetitive control together push down the error spectra and make the shapes relatively flat.

It is also interesting to observe the steady state profiles traced by the laser beams for these various cases, which are shown in Fig. 9 over 100 cycles. Here the contour traced by the LTI (ie. the integrator loop) feedback is also shown for comparison. Clearly adaptive or repetitive control substantially increases the tracking bandwidth and traces the diamond shape closely. The profiles generated by the adaptive control have significant overshoots near the vertex of the diamond but they are not present in the repetitive control. On the other hand, when the disturbance is present, the adaptive control generates profiles with much less variations than those of the repetitive control. The synergy of combining both control schemes to generate the precise profile with minimal variations is evident from the plot.

## V. CONCLUSIONS

This paper has demonstrated control of a laser-beam steering experiment for optimal random jitter rejection and

deterministic trajectory tracking. For random disturbance rejection, the high order adaptive controller based on the recursive-least-squares lattice filter achieves the experimental performance approximates the performance theoretically achievable by an optimal  $H_2$  controller based on perfect *a priori* knowledge of the plant and jitter statistics. The adaptive controller requires an estimated model of the plant but no *a priori* information about the jitter. For the periodic reference trajectory tracking, the repetitive control based on the internal model principle and robust control design achieves the experimental performance close to asymptotic perfect tracking. The repetitive controller requires an estimated model of the plant and the knowledge of the reference signal's period but no *a priori* information about the trajectory. The combined adaptive and repetitive control structure has the feature that each controller is designed based on the plant model and as such is independent of each other and has the ability to reject the random disturbance and track deterministic reference input.

## REFERENCES

- [1] Roger M. Glaese, Eric H. Anderson, and Paul C. Janzen, "Active suppression of acoustically induced jitter for the airborne laser," in *Proc. SPIE, Laser Weapons Technology*, vol. 4034. SPIE, July 2000, pp. 151–164.
- [2] Mark A. McEver, Daniel G. Cole, and Robert L. Clark, "Adaptive feedback control of optical jitter using Q-parameterization," *Optical Engineering*, no. 4, pp. 904–910, April 2004.
- [3] L. P. Fowler and R. Blankinship, "Experimental adaptive filtering and disturbance feedforward approach for flexible beam train control with single disturbance path," in *2006 Directed Energy Systems Symposium: Beam Control Conference*. DEPS, March 2006.
- [4] Byung-Sub Kim, Steve Gibson, and Tsu-Chin Tsao, "Adaptive control of a tilt mirror for laser beam steering," in *American Control Conference*. Boston, MA: IEEE, June 2004.
- [5] Néstor O. Pérez Arancibia, Steve Gibson, and Tsu-Chin Tsao, "Adaptive control of MEMS mirrors for beam steering," in *IMECE2004*. Anaheim, CA: ASME, November 2004.
- [6] Néstor O. Pérez Arancibia, Neil Chen, Steve Gibson, and Tsu-Chin Tsao, "Adaptive control of a MEMS steering mirror for suppression of laser beam jitter," in *American Control Conference*. Portland, OR: IEEE, June 2005.
- [7] M. Tomizuka, T.-C. Tsao, and K.-K. Chew, "Analysis and synthesis of discrete-time repetitive controllers," *ASME Journal of Dynamic Systems, Measurement, and Control*, vol. 111, pp. 353–358, 1989.
- [8] T.-C. Tsao and M. Tomizuka, "Robust adaptive and repetitive digital tracking control and application to a hydraulic servo for noncircular machining."
- [9] J. Li and T.-C. Tsao, "Robust performance repetitive control systems," *ASME Journal of Dynamic Systems, Measurement, and Control*, vol. 123, pp. 330–337, 2001.
- [10] Néstor O. Pérez Arancibia, Neil Chen, Steve Gibson, and Tsu-Chin Tsao, "Adaptive control of a MEMS steering mirror for free-space laser communications," in *Optics and Photonics 2005*. San Diego, CA: SPIE, August 2005.
- [11] Pawel K. Orzechowski, Steve Gibson, and Tsu-Chin Tsao, "Adaptive control of jitter in a laser beam pointing system," in *American Control Conference*. Minneapolis, MN: IEEE, June 2006.
- [12] Pawel K. Orzechowski, N. Y. Chen, Steve Gibson, and Tsu-Chin Tsao, "Suppression of laser beam jitter by high-order rls adaptive control," *IEEE Transactions on Control Systems Technology*, vol. 16, no. 2, pp. 255–267, March 2008.
- [13] S.-B. Jiang and J. S. Gibson, "An unwindowed multichannel lattice filter with orthogonal channels," *IEEE Transactions on Signal Processing*, vol. 43, no. 12, pp. 2831–2842, December 1995.

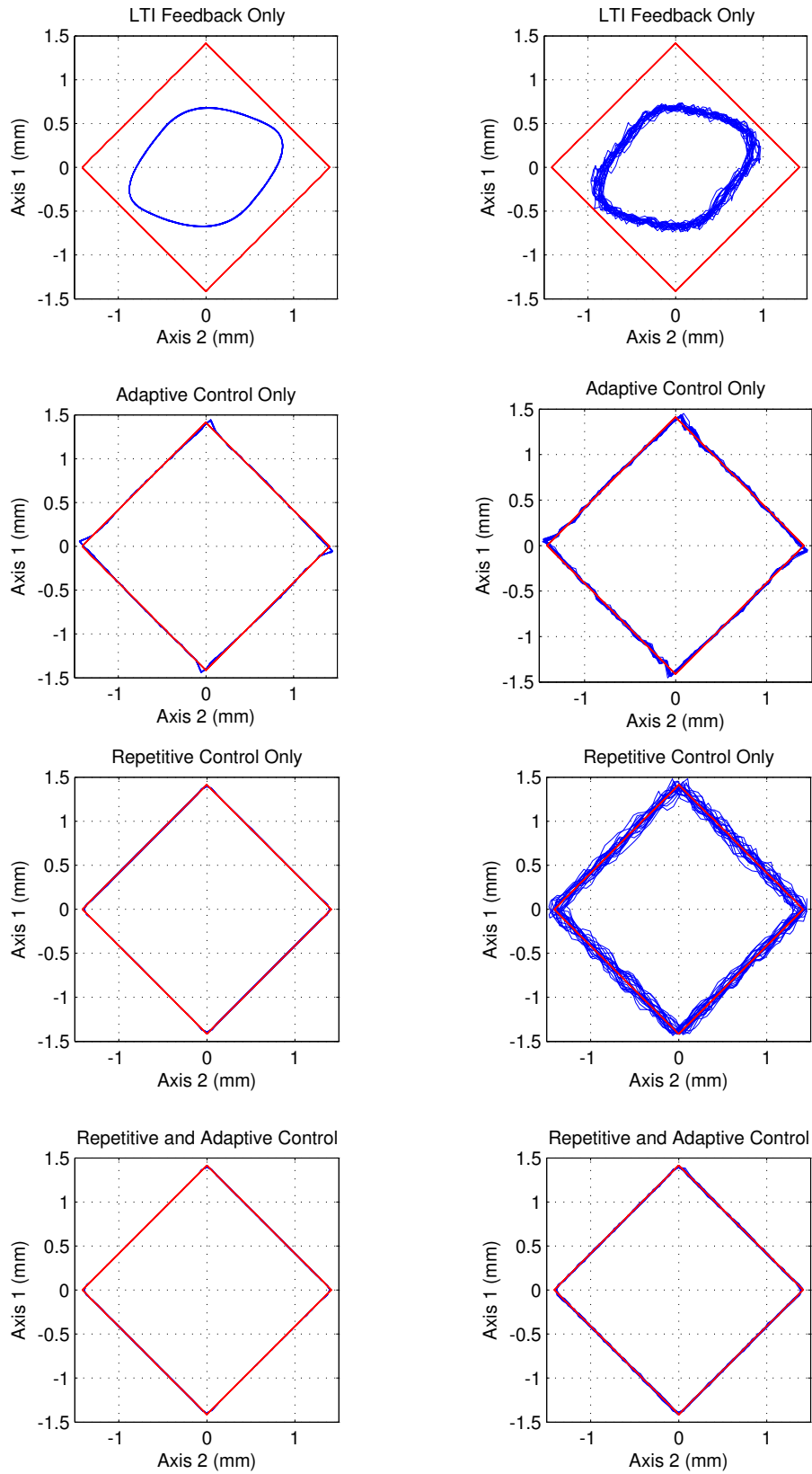


Fig. 9. Tracing a 20 Hz Diamond-shaped Contour. Steady state results for 100 cycles. The left column plots are without injected disturbances. The right column plots are with injected disturbances. From top to bottom the four cases are LTI feedback control only, adaptive control + LTI, repetitive control + LTI, adaptive control + repetitive control + LTI control